Supplementary information

Fabricating Polyacrylamide Microbeads by Inverse Emulsification to Mimic the Size and Elasticity of Living Cells

Nicholas R. Labriola, Edith Mathiowitz, and Eric M. Darling

Microbead FT-IR Analysis

The structure of 0.1% bis-acrylamide microbeads was assessed using Fourier transform infrared spectroscopy (FT-IR) with attenuated total reflectance (ATR) using a Nicolet iS50 FT-IR (Thermo Fisher Scientific, Madison ,WI, USA). Prior to scanning, the polyacrylamide (PAAm) microbeads were concentrated with centrifugation and lyophilized with a VirTis Benchtop 4K lyophilizer (SP Scientific, Gardiner, NY) for 48 hours to produce condensed, dry pellets. The spectrum of the fingerprint region (Figure S1) illustrates absorbance peaks at the expected wavenumbers for polymerized PAAm, corresponding to the flexural stretching of -NH bonds of both amide I and II (~1613 cm^{-1}), the C-N groups of both amides (~1441, 1351, and 1281 cm^{-1}), and the tensional stretching of the C=O groups of amide I (~1675 cm^{-1}).[S1]

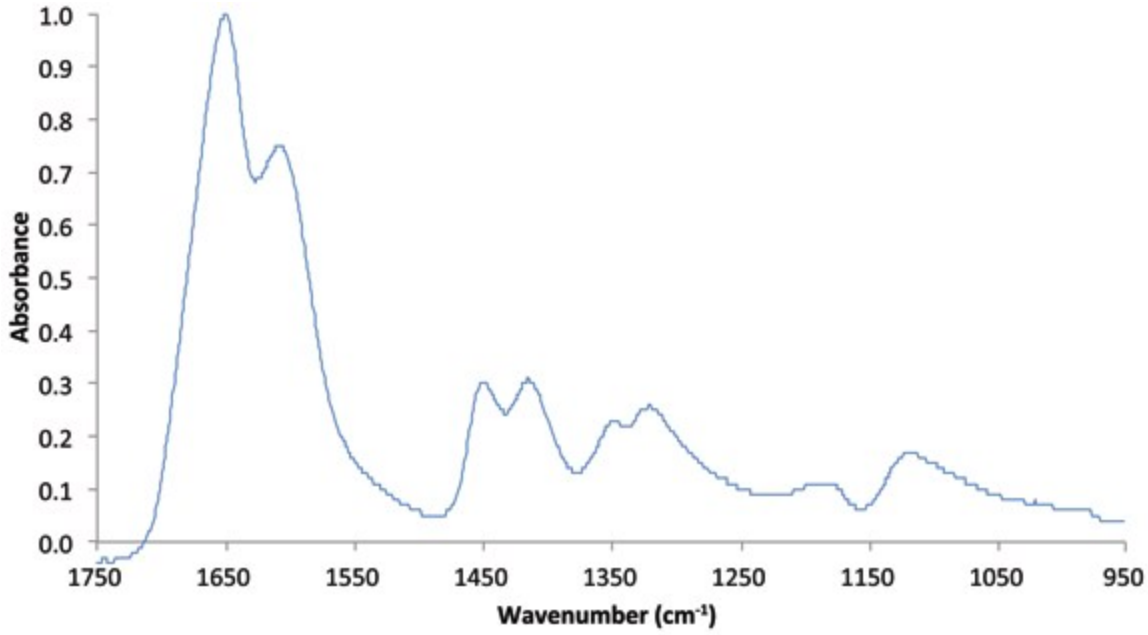

Figure S1. ATR-FTIR absorbance spectra of 0.1% bis-acrylamide microbeads. The spectrum confirms that the PAAm microbeads are polymerized polyacrylamide with absorbance peaks at the expected wavenumbers.

S1. P. Ghorbaniazar, A. Sepehrianazar, M. Eskandani, M. Nabi-Meibodi, M. Kouhsoltani, H. Hamishehkar, *Adv. Pharm. Bull.*, 2015, **5**(2), 269-275.

Batch-to-batch variability

Three sets of microbead populations were generated for two different PAAm formulations to examine variability in diameter and elastic modulus (Table S1). Microbead batches were generated using either 0.2% or 0.1% bis-acrylamide formulations with a 1500 RPM stir rate, followed by serial filtration through 100, 70, and 40 µm cell strainers. There were no significant differences in the size distributions across batches ($p > 0.4$) or formulations ($p > 0.3$) (Table S1). In general, 0.2% bis-acrylamide microbeads reliably exhibited higher elastic moduli than 0.1% bis-acrylamide microbeads; however, batch-to-batch variation in elastic moduli was significant ($p < 0.04$) (Figure S2). Due to this observation, combining multiple batches of the same formulation into a single population was avoided, since this would result in a population with a multi-modal distribution. For applications requiring microbeads of a specific elasticity, sufficient microbeads should be made in a single batch. Furthermore, that batch should be mechanically characterized to confirm the desired properties.

Additionally, paired 2D gels were generated using a 75µL sample of the PAAm solutions from each of the PAAm solutions by sandwiching the droplet between two coverslips. Once polymerized (~15 minutes @ RT), the gels were rehydrated in deionized water for 30 minutes and one of the coverslips was subsequently removed with forceps. The gels were washed three times with PBS and equilibrated for at least 1 hour before characterizing their elastic moduli with AFM. For AFM single indentation experiments, the same cantilever and indentation settings used for microbead characterization were used for the thin gels. Average elasticities were calculated from three sets of sixteen indentations (n=48) spread equally over 90x90 µm regions (Table S1).

Table S1. Batch-to-batch variation in microbead size and compliance.

Diameter: Microbeads	Batch #	0.1% bis-acrylamide	0.2% bis-acrylamide
	1	28 ± 7 µm	27 ± 8 µm
	2	29 ± 8 µm	29 ± 7 µm
	3	30 ± 9 µm	27 ± 8 µm
***$E_{elastic}$*: Microbeads**	Batch #	0.1% bis-acrylamide	0.2% bis-acrylamide
	1	720 ± 70 Pa	1920 ± 120 Pa
	2	1010 ± 150 Pa	1340 ± 150 Pa
	3	1140 ± 160 Pa	2300 ± 350 Pa
***$E_{elastic}$*: Gels**	Batch #	0.1% bis-acrylamide	0.2% bis-acrylamide
	1	2010 ± 170 Pa	4390 ± 70 Pa
	2	2240 ± 30 Pa	4050 ± 120 Pa
	3	2270 ± 250 Pa	3970 ± 150 Pa

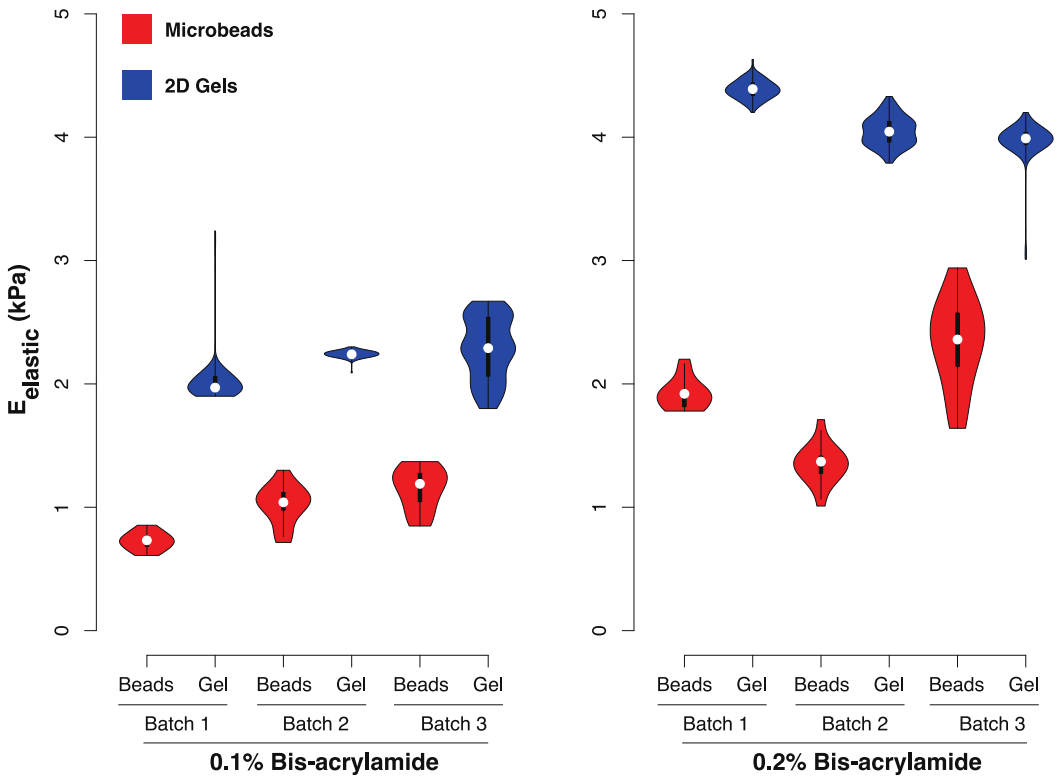

Figure S2. Batch-to-batch variation in elasticity of PAAm gels and microbeads. These violin plots illustrate the elastic moduli distributions of three batches of microbeads (red) and paired thin gels (blue) generated with 4% acrylamide and either 0.1 or 0.2% bis-acrylamide, measured with AFM. White circles represent medians, thick black lines represent 25-75% quartiles, and thin black lines represent the range of data set with outliers removed.

Fluorescent Staining of Microbeads

Fully polymerized microbeads were stained with a variety of fluorescent dyes extracted from Sharpie Liquid highlighters (summarized in Table S2) and imaged using a Nikon Eclipse Ti-U epifluorescent microscope (Nikon Instruments, Melville, NY) equipped with a QICAM 12-bit digital camera (QImaging, Surrey, BC, Canada) (Figure S3).

Table S2. Fluorescent highlighter dyes and their respective excitation/emission wavelengths.

Highlighter color	Dye contained	Excitation	Emission
Yellow	Pyrene	330 - 490 nm	440 - 545 nm
Pink	Rhodamine	530 - 560 nm	595 - 650 nm
Green	Pyrene/ Triphenylmethane	590 - 645 nm	665 - 730 nm

The fluorescence spectra of these dyes are partially dependent on pH. As such, the wavelength range of the filter cubes used to image each dye are reported. It should be noted that the green dye, which includes pyrene dye, exhibits dim fluorescence in the same channels as the yellow dye but with the addition of bright signal at longer wavelengths.

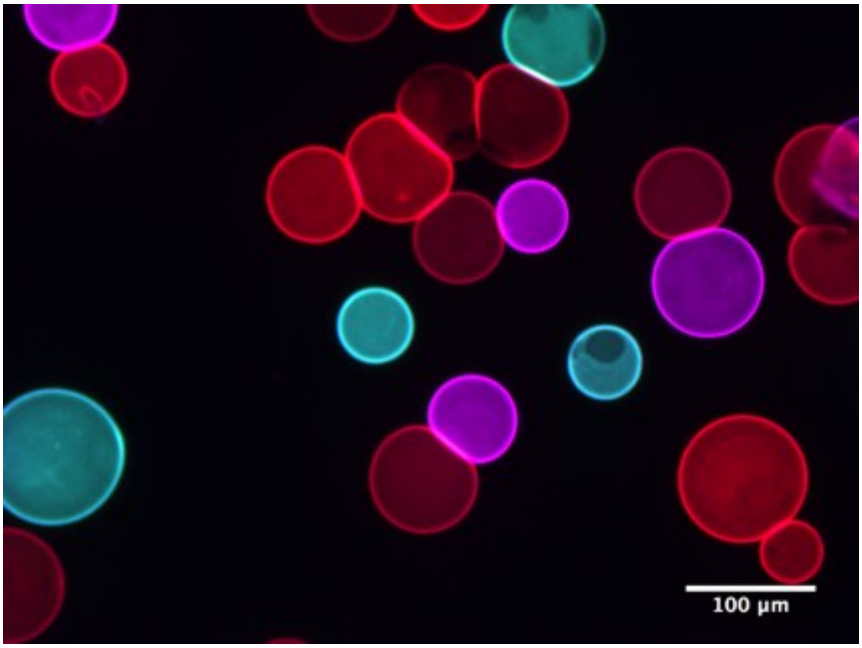

Figure S3. Microbeads stained with fluorescent dyes to allow easy visualization. Separate populations of microbeads were stained with three different fluorescent dyes to create distinct visual tags that can be used to track microbead location. Teal colored beads represent those stained with pyrene dye, pink colored beads represent those stained with a mix of pyrene and triphenylmethane dyes, and red colored beads correspond to rhodamine stained microbeads.

Microbead Size Characterization

Microbead size distributions were determined through the analysis of epifluorescent images, using ImageJ. Sixteen images of pyrene-stained microbeads were acquired using a Cytation3 Cell Imaging Multi-Mode Reader (Biotek Instruments Inc., Winooski, VT) using a 10x objective. Since fluorescence intensity was not quantified for this study, imaging parameters were optimized for each population using the auto focus and auto exposure features available through the provided software (Gen 5, version 2.05.5, Biotek). Images were loaded into Image J (version 1.47, National Institute of Health, Bethesda, MD) and converted to binary images through the application of an intensity threshold. The additional binary functions, "fill holes" and "watershed," were applied to account for lessened fluorescence intensity in the central region of microbeads and identify edges of microbeads contacting each other, respectively. The area of the particles was then assessed with the "analyze particles" feature with additional thresholding to remove the detected regions of high intensity that were less than 5 $pixels^2$ in area or less than 0.60 in circularity. Recorded areas that corresponded to out of focus microbeads were removed manually on a per image basis. The measured areas were then converted from $pixles^2$ to μm^2 using the appropriate pixel ratio associated with the imaging system. The effective diameters (in μm) were then calculated from the area measurements.

Microbead Loss during Processing

A significant percentage of the microbead populations were lost throughout the various washes and treatment stages included in the described protocol, particularly after coating with protein. Microbeads were counted with a hemocytometer to track the loss of beads from the sulfo-SANPAH and collagen-coating treatment steps, identified as the primary points of concern. As summarized in Table S3, a loss of nearly 80% of the microbeads was observed for one test case, representative of typical runs. Losses of these magnitudes should be anticipated, particularly for any application that incorporated protein coatings as a feature of the microbead.

Table S3. Microbead yield following high-loss, processing steps.

Formulation	% of Original (after Sulfo-SANPAH)	% of Original (after Collagen coating)
0.05% bis-acrylamide	68%	42%
0.1% bis-acrylamide	>99%	29%
0.2% bis-acrylamide	95%	21%